Numerical study on spontaneous ignition of direct release of pressurized hydrogen into air

J. X. Wen[1*], B. P. Xu[1], S. Dembele[1], V.H.Y. Tam[2] and S.J. Hawksworth[3]

Abstract

Spontaneous ignition of pressurized hydrogen release is of great safety concern and has recently been the subject of numerous experimental and numerical investigations. While experimental investigations are limited by the safety constraint of the laboratory itself and capacity of the facility. A validated numerical tool which can overcome this limitation can facilitate the investigations of such phenomena and give more insights on the mechanism of spontaneous ignition and link it with equipment failure time.

This paper reports on numerical study of spontaneous ignition in direct release of pressurized hydrogen into air. A mixture-averaged multi-component approach was used for accurate calculation of molecular transport. Spontaneous ignition and combustion chemistry were accounted for using a 21-step kinetic scheme. A 5th-order WENO scheme coupled with ultra fine meshes was employed to reduce false numerical diffusion.

The simulated results demonstrated that spontaneous ignition was sensitive to release pressure and hole size. If the release pressure and diameter of the release hole were sufficiently large, spontaneous ignition would first initiate at the tip of the contact surface separating the pure hydrogen from air and then was stretched by flow divergence downwards along the contact surface. As hydrogen jet propagated further downstream, the front of contact surface became wrinkled due to the Rayleigh-Taylor and shock-density layer instabilities. The distorted contact surface would increase the chemical reaction surface and enhance the mixing process. This is considered a possible factor which may lead the spontaneous ignition to develop into a turbulent jet flame. Further study also demonstrated that the rupturing process of the initial pressure boundary played an important role; and that the presence of an obstacle near the exit could potentially quench the ignition.

Keywords: Hydrogen, High-pressure jet, Spontaneous ignition, Diffusion Ignition, Shock and Molecular Transport.

[1]Faculty of Engineering, Kingston University, Friars Avenue, London, SW15 3DW, UK
[2]EPTG, bp Exploration, Chertsey Road, Sunbury-on-Thames, TW16 7LN, UK
[3]Health and Safety Laboratory, Harpur Hill, Buxton SK17 9JN, UK
Corresponding author: j.wen@kingston.ac.uk, Tel. +44(0)2085477836, Fax. +44(0)2085477992

1. Introduction

Hydrogen is well known for its tendency to autoignite. In some accidental scenarios, pressurized hydrogen release was found to have ignited when there was no clearly identifiable ignition source [1]. Based on the analysis of the Hydrogen Accidental Database compiled by the authors, nearly 60% of the incidents were ignited for no apparent reasons. Although several ignition mechanisms have been postulated and examined in the literature [1,2], there still lacks clear understanding about the ignition mechanisms of pressurized hydrogen release. Among the postulated mechanisms, the reverse Joule-Thomson effect has been ruled out while diffusion ignition has been observed in some experiments [2-5], theoretical and numerical investigations [6-8].

The terminology of diffusion ignition was first proposed by Wolanski and Wojciki [3] following their experimental study in which pressurized hydrogen was directly released into ambient oxidizer. The release produced a strong shock wave which triggered ignition even though the overall temperature of hydrogen was below its spontaneous ignition temperature. It was suggested that ignition was caused by a temperature increase of the combustible mixture due to mass and heat diffusion between hydrogen and shock-heated oxygen.

Dryer et al. [2] experimentally demonstrated diffusion ignition of compressed hydrogen release into air. The laboratory tests involved rapid rupture of burst disks under different release pressures and downstream internal geometries. Spontaneous ignition was observed in cases with release pressures from 20 bar upwards. The internal geometry downstream of the burst disk was also found to have strong influence, especially for relatively lower release pressures. The rupture of the burst disks resulted in multi-dimensional transient flows involving shock formation, reflection and interactions. The multi-dimensional shock-boundary and shock-shock interactions significantly reduced the mixing time necessary for spontaneous ignition to occur.

Golub et al. [4] and Mogi et al. [5] experimentally investigated the shock-induced ignition of pressurized hydrogen release through a tube section. Their experiments revealed that the minimum required release pressure for spontaneous ignition to occur was dependant on the tube length. As the tube length was increased, the minimum release pressure required to trigger spontaneous ignition was found to drop. Liu et al. [6] conducted two-dimensional numerical simulations of spontaneous ignition of pressurized hydrogen directly released into ambient air. They examined three extremely high pressure releases into an open ambient environment through a small hole with a diameter of 1 mm. Their results showed that spontaneous ignition occurred at the tip region of the contact surface separating hydrogen and air after 10μs for the 40 and 70MPa cases. However, the local combustion was quenched quickly due to the cooling effect from flow divergence.

Radulescu and Law [7] investigated the initial transient hydrodynamic evolution of highly under-expanded jets. Two-dimensional numerical simulations were conducted to study the flow field during the initial release stage. The predictions revealed that the jet front was laminar at the initial stages following the release. It was also found that the frontal jet interface was susceptible to both Rayleigh-Taylor and shock-density layer instabilities, which can enhance the ignition process of the entire jet and lead to the establishment of turbulent jet fames.

In our previous studies [8,9], spontaneous ignition of high pressure hydrogen releases was numerically demonstrated for a release through a tube section as well as direct release into

an ambient environment. A second order upwind numerical scheme and a steady supersonic inflow boundary condition were employed in these studies. To reduce numerical diffusion, the contact surface was tracked using an ALE (Arbitrary Lagrangian-Eulerian) approach.

In this paper, the numerical scheme is improved to high order WENO (weighted essentially non-oscillatory) scheme to reduce numerical diffusion and the damping of the instabilities at the contact surface. The computational domain is also extended into the high-pressure tank to better capture the highly transient process of the release.

Finally it should be pointed out that the sudden release, reported in our previous studies, represent an idealized scenario. In practice, bursting disks used in experiments would take a finite amount of time to open and equipment also has different failure time and mode. A parametric study is therefore conducted to clarify the influence of pressure boundary rupture rate on the possibility of spontaneous ignition. The effect of rupture rate of the pressure boundary and obstacle close to the release exit are also investigated.

2. Numerical methods

Numerical study of diffusion ignition is of great challenge. As the release flow contains strong shock waves (see Fig. 1b), DNS would be desirable but is prohibitive due to its inherent limitations at high Reynolds numbers and the constraint of current computing power. Traditionally for supersonic flows, the Euler equations are solved, neglecting the diffusion terms. However, the mixing at the contact surface through molecular diffusion is crucial to the present study. As such the diffusion terms in the Navier-Stokes (N-S) equations have to be considered. We have, therefore, decided to use the Implicit Large Eddy Simulation (ILES) approach [10-12], which is based on the hypothesis that the action of sub-grid scales on the resolved scales is equivalent to a strictly dissipative action. In this method, the N-S equations are implicitly filtered by the discretization and the implicit dissipative truncation error from the numerical scheme for the convection terms is regarded as an adaptive numerical dissipation to model the unresolved small scales in the same manner as an explicit sub-grid scale model. Due to shock induced discontinuity, the hydrogen-air contact surface involves steep gradients of species. An explicit sub-grid scale model would bring an excessive numerical diffusion to falsely enhance the mixing at the contact surface and the ILES method could inherently circumvent this problem.

Molecular diffusion across the contact surface is a very slow process compared to the very short ignition delay time. To prevent excessive false numerical diffusion to smear the real physical diffusion at the contact surface, a 5^{th}-order upwind WENO scheme [13,14] coupled with an extremely fine mesh was employed. For applications involving rich structures such as the highly under-expanded release flow, the high-order WENO shock-capturing schemes are more efficient than low order schemes and produce lower false numerical diffusion [15].

Considering the symmetric nature of the problem, the 2-D unsteady N-S equations of a chemically reactive multi-component mixture of ideal gases are solved. The numerical schemes are based on the ALE method [16] in which convection terms are solved separately from the other terms. Each time cycle is divided into two phases: a Lagrangian phase and a rezone phase. In the Lagrangian phase, a second-order Crank-Nicolson scheme is used for the diffusion terms and the terms associated with pressure wave propagation, a 3^{rd} -order total variation diminishing (TVD) Runge-Kutta method [14] is used in the rezone phase to solve the convective terms. The coupled semi-implicit equations in the Lagrangian phase are solved by a SIMPLE type algorithm with individual equations solved

by conjugate residual method [17]. For spatial differencing, a 5th-order upwind WENO scheme is used for the convection terms and the second-order central differencing scheme is used for all the other terms.

A mixture-averaged multi-component approach [18] was used for accurate calculation of molecular transport. For spontaneous ignition chemistry, Saxena and Williams' detailed chemistry [19] scheme which involves 21 elementary steps among 8 reactive chemical species was used. Third body reactions and reaction-rate pressure dependant "falloff" behavior are considered in the chemistry. Since pressurised hydrogen release undergoes strong under-expansion after discharging into an open space, a detailed chemistry allowing for the pressure dependant reaction rate is beneficial to accurately simulate the hydrogen spontaneous ignition phenomenon.

3. Problem description

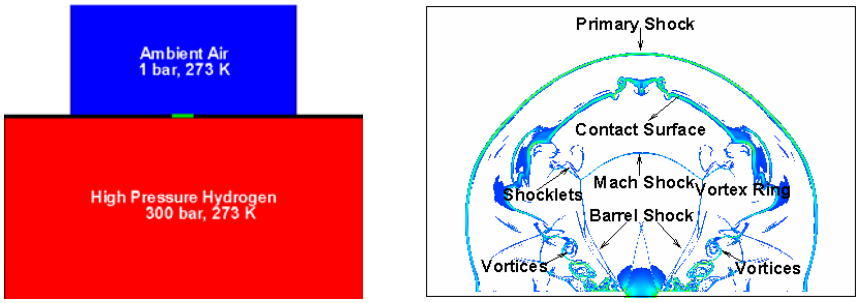

Fig. 1 a. Computational domain (left) and b. typical release flow structures (right)

The computational domain is schematically shown in Fig. 1a and typical release flow structures are also shown in Fig. 1b using the predicted density Schlieren from the release case of 100bar through a 5mm hole at t=40μs. It is composed of three cylindrical regions: pressurised vessel (in red), release hole (in green) on the vessel wall (in black) and ambient environment (in blue). All the simulations were started from still with the computational domain filled with ambient air and pure highly pressurized hydrogen separated by a thin film at the bottom plane of the hole. All the solid walls were assumed to be non-slip and adiabatic. The computational grids were clustered around the release hole and its axis. The key parameters of the release scenarios considered are listed in Table 1.

Table 1 Computational parameters

Parameters	Value
Release pressure P(bar)	100 ~ 300
Initial Temperature (K)	273
Diameter of hole D(mm)	1 ~ 5
Thickness of the wall (mm)	0.5
Minimum grid spacing (μm)	10

4. Results and analysis

4.1 Prediction of thickness of contact surface

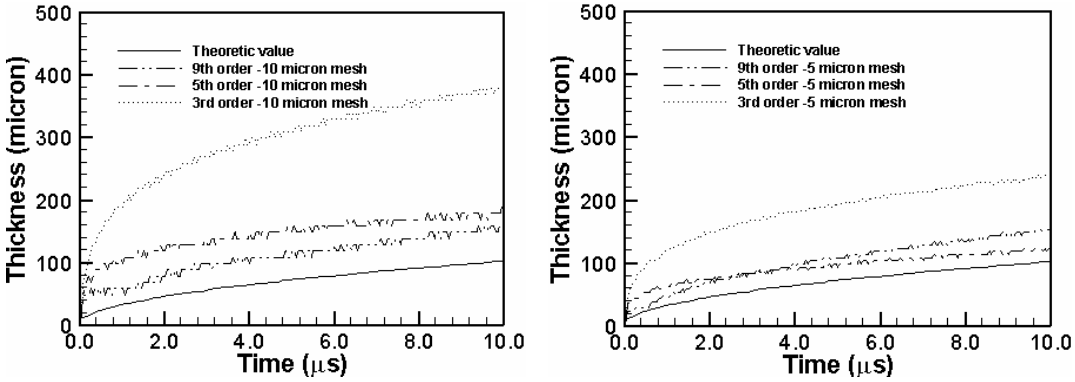

Fig. 2 Comparison of predicted thicknesses of contact surface for 1-D release case (left for 10 micron mesh and right for 5 micron mesh)

Numerical study of diffusion ignition is extremely challenging due to the substantial scale difference between diffusion and advection. To prevent molecular diffusion to be smeared out by numerical diffusion from the discretization of advection terms, high order numerical schemes along with fine grid resolution are required. Before 2-D simulations were conducted, the theoretic thickness of contact surface which is defined as the depth of the mixing region with a molar fraction of hydrogen between 1% ~ 99%, was firstly predicted by numerically solving multi-component diffusion equations of species and energy by a fourth order Runge-Kutta method and the results are presented in Figure 2.

The diffusion computation was performed for a 1-D domain filled with still hydrogen and air, so there was no numerical diffusion from convection terms in this case and the results can be regarded as an exact value for comparison. The initial conditions were taken from a 1-D test release case of 300bar, in which a close-end shock tube was filled with high-pressure hydrogen and ambient air separated by a diaphragm situated in the middle of the tube. The pressure was assumed to be 36bar (local pressure at the contact surface) across the 1-D domain and initial air temperature was 2000K (shock-heated air temperature) and initial hydrogen temperature was 150K (expanding hydrogen temperature). The thickness of contact surface was time-dependant and about 70 microns at t=5μs and 100 microns at t=10μs respectively. In order to investigate the required resolution for the mixing at the contact surface, the 1-D release case was simulated for two grid resolutions using three different order WENO schemes and the results are also listed in Figure 2. The predictions were found to be dependant on grid resolution and accuracy order. It was found that the 9^{th} –order scheme led to some oscillations at the contact surface, while the 5^{th}-order and 3^{rd}-order schemes were relatively stable. However, the 3rd-order scheme also produced excessive numerical diffusion. Comparing to the theoretic value of 100 microns, the contact surface thicknesses predicted by the 5^{th}-order scheme were 125 microns from the 5 micron mesh and 180 microns from the 10 micron mesh, respectively. The 5 micron mesh is quite expensive even in 2-D. Therefore, a more affordable mesh size of 10 microns was chosen for our simulations. With this resolution, numerical diffusion can not be totally excluded, but it can be used to model unresolved/unaccounted turbulent mixing e.g. from rupture of

pressure boundary as stated by Dryer et al [2] by employing implicit large eddy simulation approach [10-12], which is based on the hypothesis that the action of sub-grid scales on the resolved scales is equivalent to a strictly dissipative action as discussed in Section 2.

4.2 2-D Simulations of direct release into ambient air

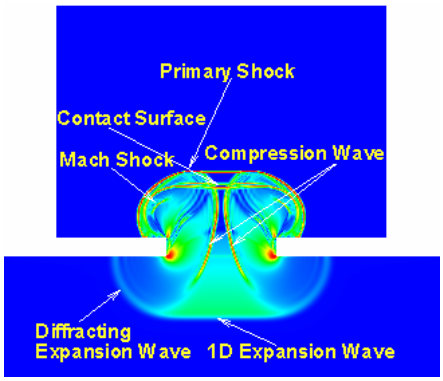

Fig. 3 Typical flow structures of the very early release stage

Both our predictions as well as experimental observation [3] suggest that spontaneous ignition occurs in the very early stage of the release. In this stage, the flow is highly transient and its characteristics play an important role in the occurrence of spontaneous ignition. Typical flow structures are shown in Fig. 3 using the predicted density Schlieren, while the transient flow evolution is illustrated through a series of snapshots in Fig. 4 using contours of density Schlieren and temperature at a time interval of 0.8μs for a release pressure of 200bar through a 3mm hole. Upon release, a one-dimensional expansion wave was established and developed into the high-pressure hydrogen. Meanwhile, a strong one-dimensional normal shock was generated and propagated into the air. Expansion waves were also initiated around the upper edge of the hole. Owing to the expansion, the frontal area of the normal shock was reducing until a "critical shock" [20], which was the first semi-spherical primary shock, was reached. The critical shock was essentially the shock wave that first became fully non-planar. Before the critical shock was formed, the strength of the normal shock almost remained constant [21]. The semi-spherical shock lost its strength rapidly after the formation of the critical shock. It can be seen in Fig. 4 that the temperature of the shock-heated air nearly remains constant prior to the critical shock and then it drops quickly due to flow divergence. Since the temperature drops quickly after the formation of the critical shock, spontaneous ignition could only occur prior to the disappearance of the normal shock otherwise the initial combustion would soon be quenched by flow divergence. The delay time for the formation of the critical shock is related to the release pressure and the diameter of the hole, but mainly determined by the latter [21]. It is expected to be much longer for releases through larger holes. Therefore, there is much longer mixing time for releases through larger holes and more chances for spontaneous ignition to initiate.

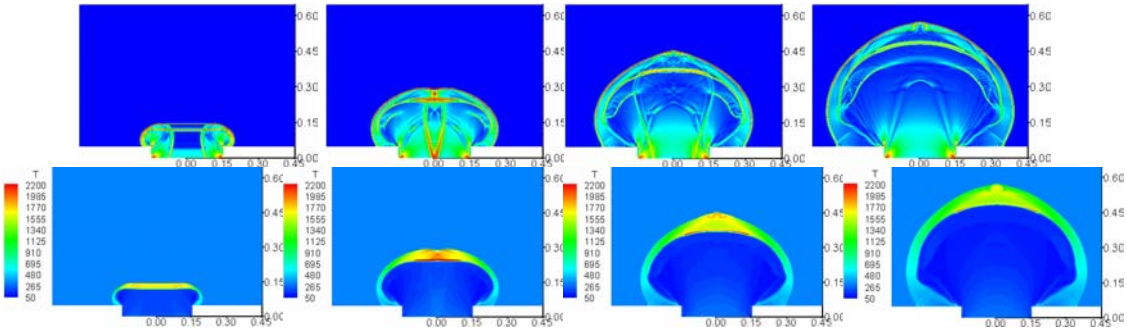

Fig. 4 Contours of density Schlieren and temperature at a time interval of 0.8μs for the 200bar release through a 3mm hole

Owing to the high lateral expansion of hydrogen originating at the upper hole edge, another important shock wave, Mach shock, was initially formed near the upper edge within the expanding hydrogen and gradually evolved into an integral semi-spherical shock at the centre. There also exists a very strong compression wave which was induced by the constraint of the hole on the expansion initiated at the lower edge. The shock-heated air was further heated by the compression wave and a hot spot was generated when the compression wave merged at the axis. The disturbance of the compression wave could facilitate turbulent mixing by amplifying the instabilities at the contact surface.

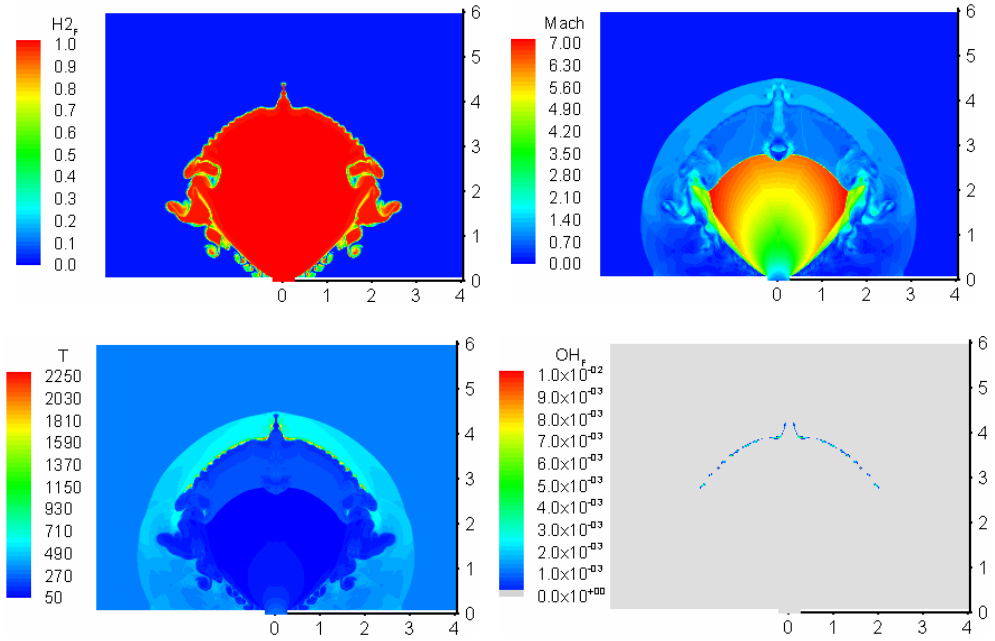

Fig. 5 Contours of hydrogen mass fraction, Mach number, temperature and OH mass fraction for a release case of 300 bar through a 5mm hole at t=40μs

To gain an overview of the flow structure of the under-expanded hydrogen jet, a simulation was run for a release case of 300bar through a 5mm hole. Typical flow structure of under-expanded hydrogen jet is shown in Fig. 5. If the release pressure and the hole size are sufficiently large, there would be sufficient mixing time for mass and energy transfer

between the shock-heated air and the under-expanded hydrogen at the contact surface through diffusion and lead to a sharp increase in the temperature of the flammable mixture which would autoignite before the significant temperature drop after the critical shock. Spontaneous ignition would first initiate at the tip of the contact surface and then was stretched by flow divergence downwards along the contact surface. As the hydrogen jet propagated further downstream, the front of the contact surface became wrinkled due to the Rayleigh-Taylor and shock-density layer instabilities. The distorted contact surface would increase the chemical reaction surface and enhance the mixing process. This is considered a possible factor for the spontaneous ignition to develop into a turbulent jet flame.

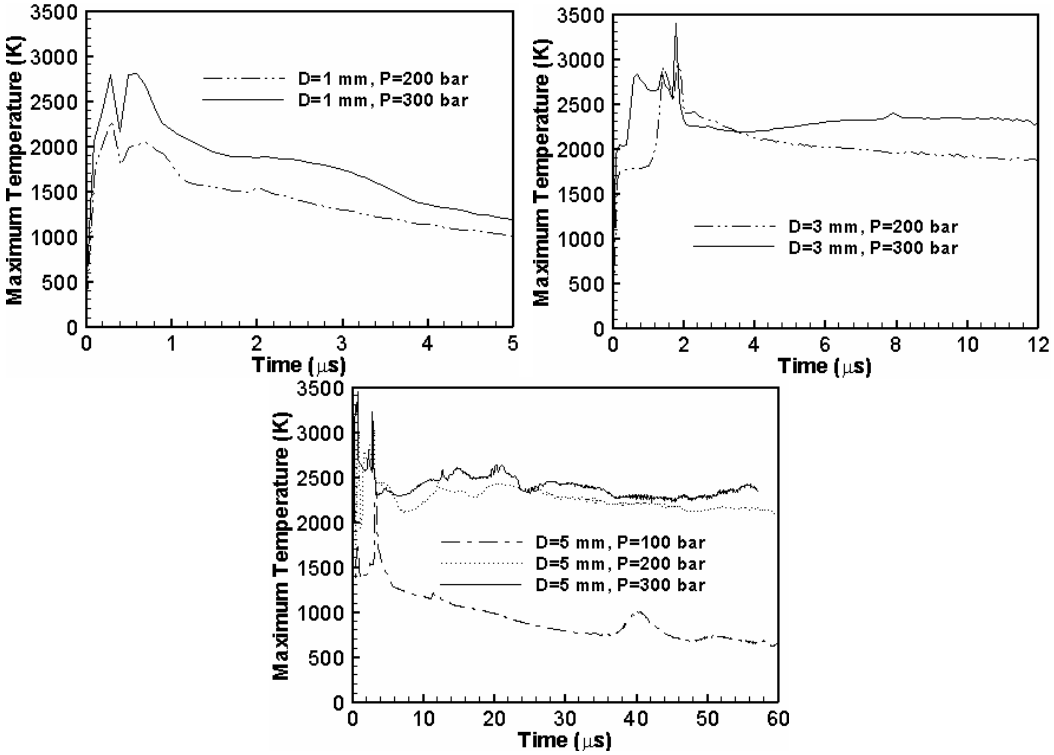

Fig. 6 Maximum temperature versus time for releases through different hole sizes under different release pressures

Fig. 6 shows maximum temperature variation with time for releases through different hole sizes under different release pressures. For releases through the 1mm hole, spontaneous ignition did not occur for the 100 bar case. Although the two high temperature peaks in the 200 and 300 bar cases suggest that spontaneous ignition did occur, the maximum temperature drops quickly indicating that flame was quickly quenched due to flow divergence. When the diameter of the hole is increased to 3mm, spontaneous ignition takes place in both the 200 and 300 bar cases. This is most likely due to the longer mixing time before the formation of the critical shock as discussed above. It is also seen that the temperature history of the 200bar case is showing the trend of the flame being gradually quenched. This could be because the initial flame was not wide enough and hence did not generate sufficient heat release to overcome flow divergence. For the release cases through a 5mm hole, it is seen that for both the 200 and 300 bar cases, spontaneous ignition occurred and the flames remained still stable at t=60μs with temperatures around 2250 K.

However, for the case of 100bar, although spontaneous ignition did occur, the flame is quickly quenched by the diverging flow.

4.3 The effect of rupture rate of initial pressure boundary

The effect of rupture rate of initial pressure boundary on spontaneous ignition of direct release was studied by simulating a release pressure of 300bar through a hole with a diameter D=3mm. To simulate the rupture process of the pressure boundary, a thin film with a thickness of 0.1mm was placed at the bottom plane of the release hole. As simulations started, the thin film was ruptured from the centre at controlled rates. Five rupture times were simulated, 0.0μs, 0.3μs, 0.6μs, 0.9 μs and 1.2 μs respectively. A rupture time of 0.0 μs corresponds to the sudden release case.

Fig. 7 shows the contours of pressure at the very early release moments with a time interval of 0.6 μs. As the pressure boundary ruptured gradually, the initial leading shock was not normal any more and the pressure behind the shock dropped more quickly for a slower rupture rate due to expansion. The slower the rupture rate was, the quicker the expansion in the process of rupture. For the rupture time of 1.2 μs, the early expansion was sufficiently high to produce a Mach shock inside the expanding hydrogen at the front of the hydrogen jet and the leading shock gradually turned to be nearly flat. The pressure between the flat leading shock and Mach shock remained almost constant due to lack of flow divergence in the release direction. The development of the above mentioned compression wave was also delayed and its strength weaker due to the longer rupture time.

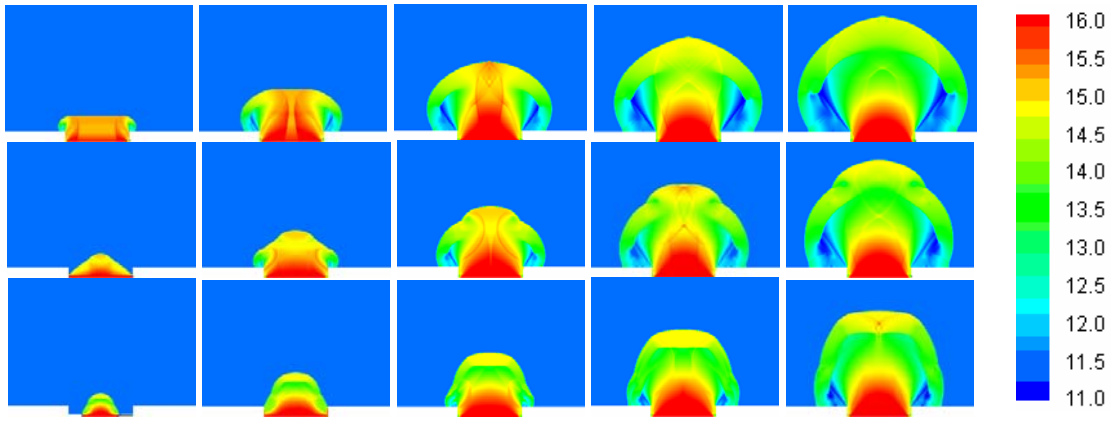

Fig. 7 Contours of local pressure (bar) during the very early release stage at an interval of 0.6 μs. (top line: sudden rupture; middle line: rupture time of 0.6 μs; bottom line: rupture time of 1.2 μs)

The contours of temperatures and OH mass fraction are shown in Fig. 8. For the case with a rupture time of 0.6 μs, a visible flame can be seen at the tip of the jet. However, the flame was narrower and could hardly spread downwards. The width of the initial flame was found to increase with the rupture rate. For the case of rupture time of 1.2 μs, no flame was observed due to the insufficient shock-heated air temperature resulting from the earlier expansion. The OH mass fraction was as low as 1.4×10^{-6} at t=8.0μs for this case.

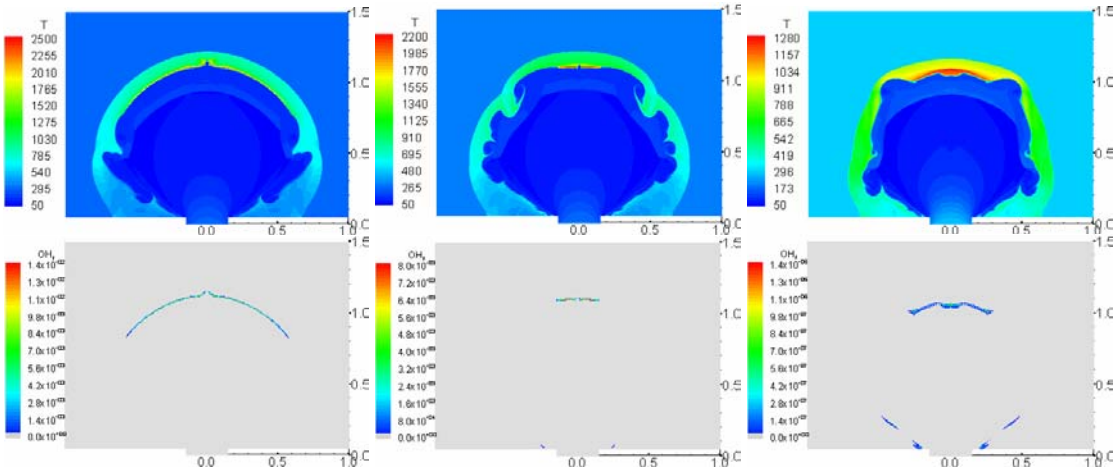

Fig. 8 Contours of temperature and OH mass fraction at t=8μs for rupture time of 0 μs (left), 0.6 μs (middle) and 1.2 μs (right)

Fig. 9 plots the maximum temperature variation with time for the five simulated cases. For the case of sudden rupture, the air was shock-heated to 2000K upon release and the maximum temperature jumped to 2800K from t=0.2μs due to spontaneous ignition. The flame temperature stayed nearly constant prior to the disappearance of the normal shock. At t=1.8μs, the temperature reached as high as 3700K due to strong compression from the compression wave. The maximum temperature then dropped sharply to 2300K because of expansion and increased slightly as the flow divergence slowed down. For the other cases, the air was also shock-heated to around 2000K upon release and then the temperature started to drop due to expansion. As the temperature dropped to certain values, it jumped again. Examination of the detailed temperature fields show that this is caused by local combustion at the exit around its edge. This local combustion was quickly quenched and the maximum temperature dropped again sharply. Following this, for the rupture times of 0.3 μs and 0.6 μs, the temperature picked up again due to spontaneous ignition and then stabilized at around 2300K. For the rupture times of 0.9 μs and 1.2 μs, the shock-heated temperature dropped quickly to a lower value which was not sufficiently high to initiate an ignition within the very short time period before the temperature decreased gradually due to flow divergence. A slow increase in the temperature for the rupture time of 0.9 μs from t=2 μs was due to the delayed further heat-up by the compression waves.

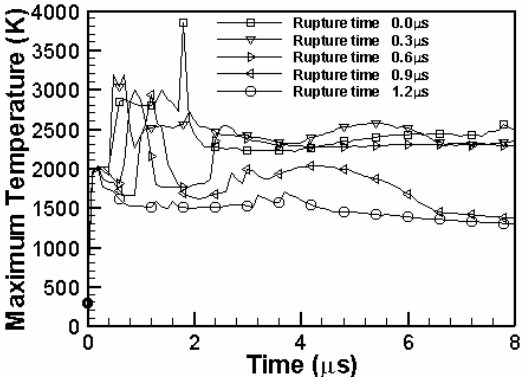

Fig. 9 Maximum temperature versus time

4.4 The effect of an obstacle close to the exit

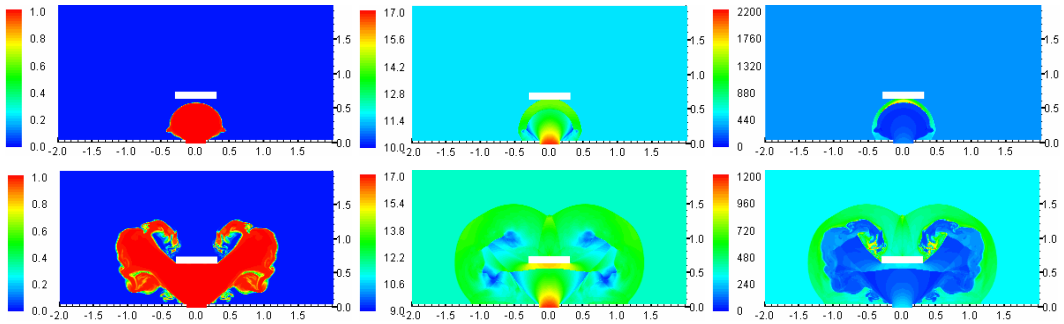

Fig. 10 Contours of hydrogen mass fraction, pressure and temperature for the release pressure of 300bar at t=3.5 μs (top) and t=15 μs (bottom).

The effect of an obstacle close to the exit was studied by simulating releases of two different release pressures through a hole with a diameter D=3mm. The obstacle was 6mm wide sited at a distance of 6mm from the exit. Contours of hydrogen mass fraction, pressure and temperature for the release pressure of 300bar at two different release moments are shown in Fig. 10. It was found that ignition occurred before the hydrogen jet impinged on the obstacle. The jet front then hit the obstacle's lower surface and changed its direction to form a wall jet. The pressure built up to a high value at the impingement region and a shock structure similar to Mach shock was formed just below the obstacle. Ahead of the shock wave, the flow was decelerated to subsonic level. As the wall jet passed by the obstacle, diffraction waves were formed at the lower outer edge of the obstacle. Once the flame reached the lower surface of the obstacle, it started to follow the wall jet propagating along the surface. As it passed the corners of the obstacle, the flame was quenched by the cooling effect from the diffraction waves. Although the obstacle could enhance the mixing process by promoting turbulence, the flame could not survive while passing the obstacle due to the quenching effect.

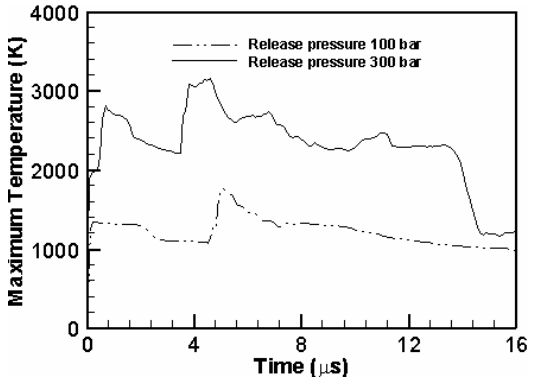

Fig. 11 Maximum temperature versus time

The maximum temperatures are plotted in Fig. 11 for two different release pressures. For the 300 bar case, the air behind the leading shock wave was quickly heated to around 2000K. It soared up to 2800K following spontaneous ignition. Afterwards the flame

temperature started to drop due to flow divergence. When the flame reached the lower surface of the obstacle, its temperature increased sharply again at the stagnation region and then started to drop again as the flow was bounced back by the surface. The flame on the lower surface survived a period of time until it was quenched at t=14 μs. For the 100 bar case, the air was only shock-heated to 1360K, which was insufficient to initiate an ignition prior to the disappearance of the normal shock. When the jet reached the lower surface, its temperature increased to 1760K and started to drop due to flow deceleration after the shock wave behind the surface.

5. Concluding remarks

Numerical investigations have been conducted on spontaneous ignition of direct release of pressurized hydrogen. The predictions demonstrated that spontaneous ignition was sensitive to release pressure and hole size. If the release pressure and diameter of the release hole were sufficiently large, spontaneous ignition would first initiate at the tip of the contact surface separating the expanding hydrogen from shock-heated air. The flame was then stretched by flow divergence downwards and outwards along the contact surface. As the jet propagated further downstream, the front of the contact surface became wrinkled due to the Rayleigh-Taylor and shock-density layer instabilities. The distorted contact surface would increase the chemical reaction surface and enhance the mixing process. This is considered a possible factor for spontaneous ignition to develop into a turbulent jet fire.

The study also demonstrated that the rupturing process of the pressure boundary, which could represent the bursting disk in spontaneous ignition tests, play an important role in spontaneous ignition. Compression waves are formed during the rupturing process which can further heat the air behind the leading shock. When the rupture rate slows down, the leading shock weakens and the hydrogen at the contact surface is heated to a lower temperature. Below a critical value of the rupture rate, the ignition delay time becomes longer than the period before the temperature of the hydrogen decreases due to flow divergence. In such case, no spontaneous ignition would occur.

Finally, some preliminary study with an obstacle in front of the jet close to the exit indicates that the obstacle has an effect of quenching the flame quickly soon after the spontaneous ignition. However, in this particular preliminary investigation, we did not consider the hear capacity of the obstacle. It is postulated that if the obstacle's heat capacity is large, its temperature is unlikely to rise much within the extremely short time period. The present simulation actually mimic this situation. On the other hand, if the obstacle's heat capacity is so low that its temperature could rise sharply during the very short period of time, then it could drop quickly as well. Hence, it is thought to be unlikely that such an obstacle would act as a hot spot above the autoignition temperature to ignite and stabilise the flame. Further study is underway for more detailed investigations on the effect of obstacles. This can potentially lead to the development of possible mitigation techniques against unwanted spontaneous ignition.

REFERENCES

1. Astbury, G.R. and Hawksworth, S.J. (2007), Spontaneous ignition of hydrogen leaks: a review of postulated mechanisms, International Journal of Hydrogen Energy, 32, 2178-2185.
2. Dryer, F.L., Chaos, M, Zhao Z. Stein, J.N., Alpert, J.Y. and Homer. C.J. (2007), Spontaneous Ignition of Pressurized Releases of Hydrogen and Natural Gas into Air, Combust. Sci. and Tech., 179,663-694.
3. Wolanski, P. and Wojcicki, S. (1972), Investigation into the Mechanism of the Diffusion Ignition of a Combustible Gas Flowing into an Oxidizing Atmosphere. Proc. Combust. Instit., 14, 1217-1223.
4. Golub, V.V. , Baklanov, D.I. , Bazhenova, T.V. , Bragin, M.V. , Golovastov, S.V., Ivanov, M.F. , Volodin, V.V. (2007), Shock-induced ignition of hydrogen gas during accidental or technical opening of high-pressure tanks, Journal of Loss Prevention in the Process Industries, in press, available on-line.
5. Mogi, T, Kim, D, Shiina, H and Horiguchi, S. (2007) Self-ignition and explosion during discharge of high-pressure hydrogen, Journal of Loss Prevention in the Process Industries, in press, available on-line.
6. Liu, Y.F., Sato, H., Tsuboi, N., Hjigashino, F., and Hayashi, A.K. (2006), Numerical simulation on hydrogen fuel jetting from high pressure tank. Sci. Tech. Energ. Mater., 67,7-11.
7. Radulescu, M.I., Law, C.K. (2007), The transient start of supersonic jets, J. Fluid Mech., 578, 331-369.
8. Xu, B.P., Hima, L.EL, Wen, J.X., Dembele, S., Tam, V.H.Y, Donchev, T. (2007) Numerical Study of Spontaneous Ignition of Pressurized Hydrogen Release through a tube into Air, Journal of Loss Prevention in the Process Industries, available online.
9. Xu, B.P., Hima, L.EL, Wen, J.X., Dembele, S., Tam, V.H.Y. (2007), Numerical Study of Spontaneous Ignition of Pressurized Hydrogen Release into Air, International Conference on Hydrogen Safety, 11-13 September 2007, San Sebastian, Spain.
10. Boris, J.P., Grinstein, F.F., Oran, E.S., Kolbe, R.L. (1992), New insights into large eddy simulation, Fluid Dynam. Res., 10,199-228.
11. Drikakis, D. (2002), Embedded turbulence model in numerical methods for hyperbolic conservation laws, Int. J. Numer. Methods Fluids, 39, 763-781.
12. Drikakis, D. (2003), Advances in turbulent flow computations using high-resolution methods, Prog. Aero. Sci., 39, 405-424.
13. Qiu, J.X. and Shu, C.W. (2002), On construction, Comparison, and Local characteristic Decomposition for High-Order Central WENO Schemes, J. of Comput. Phys. 183, 187-209.
14. Balsara, D., Shu, C.W, (2000), Monotonicity Preserving Weighted Essentially non-oscillatory Schemes with Increasingly High Order of Accuracy, J. of Comput. Phys. 160, 405-452.
15. Jang, G.S. and Shu, C.W. (1996), Efficient Implementation of Weighted ENO Schemes, J. of Comput. Phys. 126, 202-228.
16. C.W.Hirt, A.A.Amsden (1974), J.L.Cook, J. Comput. Phys. 14,227.

17. O'Rourke, P.J. and Amsden, A.A. (1986), Implementation of a conjugate residual iteration in the KIVA computer program, Los Alamos National Laboratory report LA-10849-MS.
18. Kee, R.J., Rupley, F.A. and Miller, J.A. (1989), Chemkin II: a fortran chemical kinetics package for the analysis of gas-phase chemical kinetics. Sandia National Laboratories Report No. SAND89-8009.
19. Saxena, P. and Williams, F.A. (2006), Testing a small detailed chemical-kinetic mechanism for the combustion of hydrogen and carbon monoxide, Combustion and Flame, 145:316-323.
20. Abate, G. and Shyy, W. (2002), Dynamic structure of confined shocks undergoing sudden expansion, Progress, in Aerospace Sciences, 38, 23-42.
21. Sloan, S.A., Nettleton, M.A. (1975), A model for the axial decay of a shock wave in a large abrupt area chang. J. Fluid Mech., 71, 769-794.